Non-cooperative identification of civil aircraft using a generalised mutual subspace method

Patricia López-Rodríguez , David Escot-Bocanegra , Raúl Fernández-Recio , Ignacio Bravo

Abstract: The subspace-based methods are effectively applied to classify sets of feature vectors by modelling them as subspaces. However, their application to the field of non-cooperative target identification of flying aircraft is barely seen in the literature. In these methods, setting the subspace dimensionality is always an issue. Here, it is demonstrated that a modified mutual subspace method, which uses *softweights* to set the importance of each subspace basis, is a promising classifier for identifying sets of range profiles coming from real in-flight targets with no need to set the subspace dimensionality in advance. The assembly of a recognition database is also a challenging task. In this study, this database comprises predicted range profiles coming from electromagnetic simulations. Even though the predicted and actual profiles differ, the high recognition rates achieved reveal that the algorithm might be a good candidate for its application in an operational target recognition system.

1 Introduction

Nowadays, with the secondary surveillance radar and the identification friend of foe in the civil and military aviation respectively, aircraft are able to recognise themselves upon a question from an interrogator system (normally a ground station). However, this cooperative identification procedure needs an active response from the target and in case of failure, the illuminated target might be classified erroneously or even pass unnoticed in the airspace. Non-cooperative target identification (NCTI) systems try to avoid these irregularities by acquiring the signature of the illuminated target, even if it is not aware, and further check its similarity with other pre-stored signatures. Since radar can operate at long ranges and under conditions of poor visibility or high noise, they were thought of as the best option to achieve NCTI [1, 2]. With a sufficiently wide bandwidth they can achieve high resolution in the collected data, providing target signatures with enough information to infer their structure. Great effort has been made along the years using high-resolution range profiles (HRRP) as signatures for air target identification [3–9]. A HRRP is the projection onto the radar line of sight of the radar energy scattered back by the different parts of an aircraft, thus, under the same measurement conditions, different aircraft will provide different HRRP.

In the literature, different methods for recognition based on HRRP have been applied such as: statistical modelling for HRRP data, which has been used to describe the likelihood between HRRPs [10], a noise-robust factor analysis model based on multitask learning, developed in [11], or hidden Markov models, that have been applied to radar target recognition in several studies [12, 13]. Feature selection methods and dimensionality reduction algorithms are also frequently used in NCTI, including wavelet transformation [14], algorithms based on a reconstruction model such as principal component analysis (PCA) [4], the differential power spectrum [15], linear discriminant functions [16], or singular value decomposition (SVD) [17].

The concept of principal angles [18] between two linear subspaces has been widely used for recognition and classification of sets of images [19, 20]. However, the approach has been barely applied in the frame of NCTI and thus, this possibility is explored in this paper. Here, a subspace model based on the mutual subspace method (MSM) is applied to matrices of consecutively collected range profiles in order to determine the type of aircraft the radar is illuminating.

The structure of the paper is as follows. Section 2 firstly introduces the algorithm methodology and further describes the test and training sets used in the experiments. Section 3 shows the results obtained with the proposed method and a comparison with other similar algorithms. Lastly, Section 4 presents the conclusions and future work.

2 Methodology

2.1 Mutual subspace method

The conventional subspace method (CSM) [21] is a statistical pattern recognition method where each class is represented by a subspace and the belonging to a class, namely the similarity, is determined by the angle between a vector $\boldsymbol{g}$, representing a test sample, and each subspace.

The MSM presented in [22], on the contrary, defines the similarity by the angle between two subspaces where the bases of the subspaces are calculated by the PCA. The relationship between two subspaces, D and S, is then defined by their principal angles, so called canonical angles, which are an extension of the angle between two vectors. A graphical explanation of both methods can be found in Fig. 1, where Fig. 1*a* shows how in CSM only one angle (Θ_1) is returned since the test sample is represented by one vector, and Fig. 1*b* shows that MSM returns k canonical angles corresponding to the $\boldsymbol{k}$ vectors that compose the smallest subspace.

Let $\boldsymbol{X}_D = [x_1, x_2, \ldots, x_M] \in \Re^{N \times M}$ be a matrix of feature vectors, in our experiment a matrix of HRRP of dimension $N \times M$ (assuming $N > M$), with M being the total number of profiles and N the number of samples. The set of profiles is modelled by the subspace spanned by the principal basis vectors: by applying eigen-decomposition to $\boldsymbol{X}_D\boldsymbol{X}_D^{\mathrm{T}}$ and exploiting the eigenvectors corresponding to the h_d largest eigenvalues, the basis of the

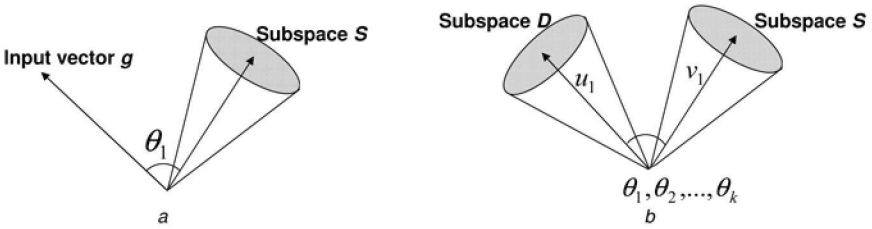

Fig. 1 *Basic concepts of subspace methods*

a Conventional subspace method (CSM)
b Mutual subspace method (MSM)

subspace D is obtained as in (1)

$$\boldsymbol{X}_D \boldsymbol{X}_D^{\mathrm{T}} = \boldsymbol{V}_D \boldsymbol{\Lambda}_D \boldsymbol{V}_D^{\mathrm{T}} \Rightarrow \hat{\boldsymbol{V}}_D \in \Re^{N \times h_d} \tag{1}$$

where $\boldsymbol{V}_D \in \Re^{N \times N}$ is a matrix containing the eigenvectors, $\boldsymbol{\Lambda}_D = \mathrm{diag}(\lambda) \in \Re^{N \times N}$ is a diagonal matrix containing the eigenvalues and $\hat{\boldsymbol{V}}_D \in \Re^{N \times h_d}$ is the selected basis of the subspace D.

As stated, the similarity measure between two subspaces D and S is defined as their canonical angles (θ_k) [23]. These are obtained recursively as

$$\cos \theta_k = \max_{\boldsymbol{u} \in D} \max_{\boldsymbol{v} \in S} \boldsymbol{u}^{\mathrm{T}} \boldsymbol{v} = \boldsymbol{u}_k^{\mathrm{T}} \boldsymbol{v}_k \tag{2}$$

such that

$$\begin{aligned} &\|\boldsymbol{u}\|_2 = \|\boldsymbol{v}\|_2 = 1 \\ &\boldsymbol{u}^{\mathrm{T}} \boldsymbol{u}_i = 0 \qquad\qquad i = 1, \ldots, k-1 \\ &\boldsymbol{v}^{\mathrm{T}} \boldsymbol{v}_i = 0 \qquad\qquad i = 1, \ldots, k-1 \\ &\quad k = 1, \ldots, \min[h_d, h_s] \end{aligned}$$

where $[\boldsymbol{u}_1, \ldots, \boldsymbol{u}_k]$ and $[\boldsymbol{v}_1, \ldots, \boldsymbol{v}_k]$ are called the canonical vectors between subspaces D and S and h_d and h_s are the number of eigenvectors taken as bases of the subspaces D and S respectively.

The canonical angles satisfy $0 \le \theta_1 \le \theta_2 \le \cdots \le \theta_k \le \pi/2$. If the columns of $\hat{\boldsymbol{V}}_D \in \Re^{N \times h_d}$ and $\hat{\boldsymbol{V}}_S \in \Re^{N \times h_s}$ define orthonormal bases for D and S respectively, then

$$\cos \theta_k = \max_{\boldsymbol{u} \in D} \max_{\boldsymbol{v} \in S} \boldsymbol{u}^{\mathrm{T}} \boldsymbol{v} = \max_{\boldsymbol{y} \in \Re^{h_d}} \max_{\boldsymbol{z} \in \Re^{h_s}} \boldsymbol{y}^{\mathrm{T}} (\hat{\boldsymbol{V}}_D^{\mathrm{T}} \hat{\boldsymbol{V}}_S) \boldsymbol{z} \tag{3}$$

considering $\|\boldsymbol{u}\|_2 = \|\boldsymbol{v}\|_2 = \|\boldsymbol{y}\|_2 = \|\boldsymbol{z}\|_2 = 1$. After the minimax characterisation of singular values given in [24] (section 8.6.1), it follows that $\boldsymbol{Y}^{\mathrm{T}} (\hat{\boldsymbol{V}}_D^{\mathrm{T}} \hat{\boldsymbol{V}}_S) \boldsymbol{Z} = \mathrm{diag}(\sigma_1, \ldots, \sigma_k)$, that is, the SVD of $\hat{\boldsymbol{V}}_D^{\mathrm{T}} \hat{\boldsymbol{V}}_S$. Thus, assuming $h_s < h_d$ and applying SVD, then

$$\hat{\boldsymbol{V}}_D^{\mathrm{T}} \hat{\boldsymbol{V}}_S = \boldsymbol{U} \cdot \boldsymbol{\Theta} \cdot \boldsymbol{V}^{\mathrm{T}} \tag{4}$$

where

$$\left.\begin{aligned} \boldsymbol{U} &= \left[\boldsymbol{u}_1, \ldots, \boldsymbol{u}_{h_d}\right] &&= \hat{\boldsymbol{V}}_D \boldsymbol{Y} \\ \boldsymbol{V} &= \left[\boldsymbol{v}_1, \ldots, \boldsymbol{v}_{h_s}\right] &&= \hat{\boldsymbol{V}}_S \boldsymbol{Z} \end{aligned}\right\} \text{canonical vectors}$$

$$\boldsymbol{\Theta} = \mathrm{diag}(\cos \theta_k) = \mathrm{diag}(\sigma_k) \quad \rightarrow \text{singular values}; \quad k = 1, \ldots, h_s$$

The similarity measure can be defined as the largest singular value $\sigma_{\max}$, as the mean of the obtained singular values, or as in here, as the squared sum of the canonical angles' cosines, that is, $S_{DS} = \mathrm{tr}(\boldsymbol{\Theta}^2)$. The higher S_{DS}, the higher the similarity between subspaces D and S. In the case that two subspaces coincide completely with each other, all canonical angles are zero and so their similarity will be $S_{DS} = k$, with k being the dimension of the smallest subspace ($k = h_s$). When the two subspaces separate, the similarity will get smaller and if the subspaces are orthogonal, it will become zero as Fig. 2 depicts.

Selecting the dimensions (h_d and h_s) of the subspaces is crucial in the classification performance. These dimensions are set taking into account the eigenvalues in $\boldsymbol{\Lambda}_D$ and $\boldsymbol{\Lambda}_S$ respectively since they reveal the information gathered by each eigenvector: the higher the eigenvalue, the higher the amount of information of the target contained in its associated eigenvector. According to this, eigenvectors with high eigenvalues will belong to a dominant subspace or *signal subspace*, containing information about the target, and those with low eigenvalues will form the *noise subspace*, containing unwanted and negligible information. If subspace dimensionality is set to a high value, then too many vectors will make up the *signal subspace*. This will cause the subspaces to be noisy, making their separability more difficult and thus, the recognition performance will be impoverished. Unfortunately, there is no theoretical way to appropriately determine the subspace dimensionality and users should tune it in advance, normally by setting an energy threshold based on the eigenvalues [4, 25].

2.2 Softweighting

In order to palliate the problem of subspace dimensionality, Kobayashi [26] introduces the concept of *softweighting* for image identification and proposes a generalised mutual subspace method (gMSM). Contrary to [26] in which gMSM is applied to static two-dimensional images for object classification, here this method is used for identification of flying aircraft from range profiles. To the authors knowledge, not only the method is used for the first time in this paper with this purpose, but also a study of the optimal selection of the softweighting parameter, which is critical for the identification and has not been done before, is carried out.

In MSM algorithm, when setting the dimensionality of a subspace, the eigenvalues take an important role: only the eigenvectors with the highest eigenvalues will be considered as basis and the rest will be discarded. The eigenvalues can be seen as if they had a binary weight (1/0) that affects the eigenvectors. A weight of 1 means that the corresponding eigenvector is a basis of the subspace and a weight of 0 means the opposite. That is, the subspace dimensionality is set based on a binary decision. Nevertheless, the eigenvalue *per se* does not take part in the

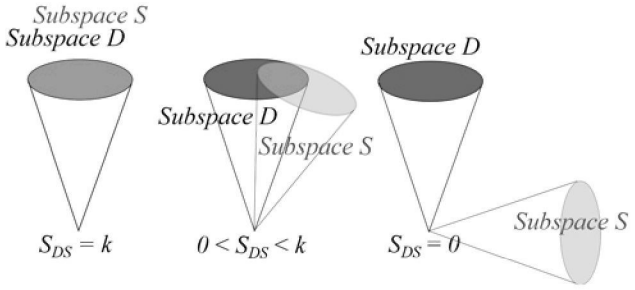

Fig. 2 *Similarity concept between subspaces*

identification algorithm, meaning that all the eigenvectors that have been chosen as basis have the same relevance in the subspace construction.

The concept of *softweighting* tries to avoid this binary decision, that is, the selection of the subspace dimension is no longer needed. *Softweighting* gives importance to all the eigenvectors, in a way that all the eigenvectors will take part in the subspace but they will be weighted by a transformed value of their corresponding eigenvalues. This transformed value is called the *softweight*. According to (1), if $\mathbf{\Lambda}_D = \text{diag}(\lambda)$ are the eigenvalues of matrix $\boldsymbol{X}_D\boldsymbol{X}_D^{\mathrm{T}}$ in descending order, the design of the *softweights* is done in consonance with these eigenvalues. Let $\mathbf{\Omega} = \text{diag}(\omega) \in \Re^{N\times N}$ be a diagonal matrix of *softweights* such that:

$$\omega = w_m(\lambda) = \min\left[\frac{\lambda}{\lambda_m}, 1\right] \tag{5}$$

where w_m is the mth eigenvalue in λ. This *softweighting* evaluates the importance of each eigenvector as a basis in the subspace by the variance relative to λ_m. The m first values of the diagonal matrix $\mathbf{\Omega}$ will be the unity and the rest will be proportionally decreasing with the mth eigenvalue. Fig. 3 illustrates the resulting *softweights* of a matrix of eigenvalues when m is set to 4 and to 1. As seen, in the dashed line, the first 4 values are equal to unity, while the rest slowly decrease proportionally to the 4th eigenvalue. On the contrary, the dotted line shows the decreasing tendency of the *softweights* in relation to the first eigenvalue.

By adding the *softweights* to (3), the importance of each eigenvector as a basis of the subspace is set. Then, the gMSM is defined as

$$\begin{aligned}\cos\theta_k &= \max_{\boldsymbol{y}^{\mathrm{T}}\Omega_D^{-2}\boldsymbol{y}=1;\, \boldsymbol{z}^{\mathrm{T}}\Omega_S^{-2}\boldsymbol{z}=1} \max \boldsymbol{y}^{\mathrm{T}}(\boldsymbol{V}_D^{\mathrm{T}}\boldsymbol{V}_S)\boldsymbol{z} \\ &\Leftrightarrow \max_{\boldsymbol{y}'^{\mathrm{T}}\boldsymbol{y}'=1;\, \boldsymbol{z}'^{\mathrm{T}}\boldsymbol{z}'=1} \max \boldsymbol{y}'^{\mathrm{T}}(\Omega_D\boldsymbol{V}_D^{\mathrm{T}}\boldsymbol{V}_S\Omega_S)\boldsymbol{z}'\end{aligned} \tag{6}$$

where $\boldsymbol{y} = \mathbf{\Omega}_D\boldsymbol{y}'$, $\boldsymbol{z} = \mathbf{\Omega}_S\boldsymbol{z}'$ and $\boldsymbol{V}_D$ and $\boldsymbol{V}_S$ are the eigenvectors as in (1). Eventually, the generalised canonical angles that define the similarity measure are computed by applying SVD to $\mathbf{\Omega}_D\boldsymbol{V}_D^{\mathrm{T}}\boldsymbol{V}_S\mathbf{\Omega}_S$, that is

$$\mathbf{\Omega}_D\boldsymbol{V}_D^{\mathrm{T}}\boldsymbol{V}_S\mathbf{\Omega}_S = \boldsymbol{U}' \cdot \mathbf{\Theta} \cdot \boldsymbol{V}'^{\mathrm{T}} \Rightarrow S_{DS} = \text{tr}(\mathbf{\Theta}^2) \tag{7}$$

As in MSM, the algorithm identifies the aircraft as the one with the highest similarity.

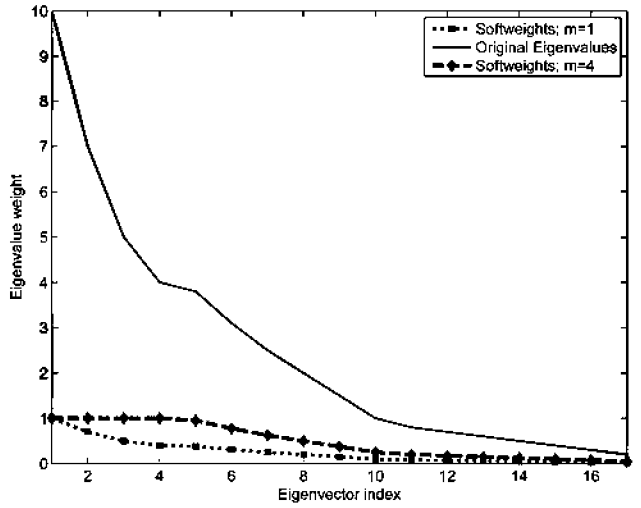

Fig. 3 *Softweighting of eigenvalues*

2.3 Datasets

In this study, we call test set to the input of our identification system and training set to the database of potential targets used to find the closest match (the output).

The test set comprises actual measurements coming from a civil aircraft measurement campaign, *ORFEO*, that took place in the Netherlands during 1995 using the FELSTAR radar (a stepped frequency S-Band radar with a bandwidth of 452.2 MHz and a nominal resolution of 0.33 m) at TNO-FEL [27]. Signatures of several targets of opportunity were acquired and information about their estimated flightpaths along with their identification was provided by a secondary radar. According to *ORFEO* specifications, the estimated aspect angles had at the most, an error of 5°, and since FELSTAR used a velocity-tolerant waveform, no velocity compensation was needed after the collection of profiles. The profiles have been amplitude normalised such that their total energy equals unity, and Hamming windowed, to reduce sidelobes that can obscure small returns at a cost of a poorer resolution. In this work, six aircraft models are considered: the Boeing 747-400, the Airbus A310, the Boeing B767-300, the McDonnell Douglas MD80, the Fokker 28, and the Fokker 100.

On the contrary, the training set, that is, the recognition database, is populated with predicted profiles, so called synthetic HRRPs. They have been obtained with the RCS-prediction code FASCRO [28], which uses high-frequency techniques (Physical Optics, PO, and Physical Theory of Diffraction (PTD)) to obtain the synthetic profiles of a certain target model at specified aspect angles. Table 1 shows the dimensions of the targets used in the experiments.

When obtaining the synthetic profiles with FASCRO, it must be noted that all electromagnetic effects that occur in a real scenario are not considered since it makes use of high frequency techniques. Moreover, the aircraft models have been developed considering every aircraft as perfect electric conductors with no protruding elements. However, since signatures of aircraft from other nations may not be available because their participation in measurement campaigns is unlikely, the use of predicted profiles as database has been opted. Besides, RCS-prediction codes allow the creation of a wide database of targets in any aspect angle just by designing their CAD models, hence, the construction and update of the database is inexpensive in contrast to measurement campaigns. Thus, as noted, due to the fact that simulations do not take into account all the electromagnetic effects that occur in a real environment, and along with CAD models not being exact replicas of real aircraft, the obtained synthetic signatures may be too ideal.

In this regard, Fig. 4 shows the differences found between the measured profile of a B767 at a certain aspect angle and the synthetic one obtained with FASCRO of the same aircraft with the same orientation. Note that the image has been zoomed in order to better appreciate these differences. Apart from the ideal scenario in which profiles are predicted, it should be remembered that the estimated aspect angles at which the real aircraft have been measured had an error of 5° at the most, so, even though the predictions have been run under the same aspect angles and, since profiles are very sensitive to it, this error may cause additional difference between actual and simulated profiles. It can also be noticed in the figure that despite both sets of profiles have been amplitude normalised, their amplitudes differ. Additionally, the measured HRRPs are noisier between peaks which also affect the amplitude normalisation.

Table 1 Synthetic aircraft dimensions

Class	Length, m	Wingspan, m	Height, m
B747	70.66	64.44	16.79
B767	54.22	47.52	14.77
A310	46.66	43.90	12.74
MD80	45.10	32.80	7.43
F100	35.53	28.08	6.58
F028	29.61	25.07	6.62

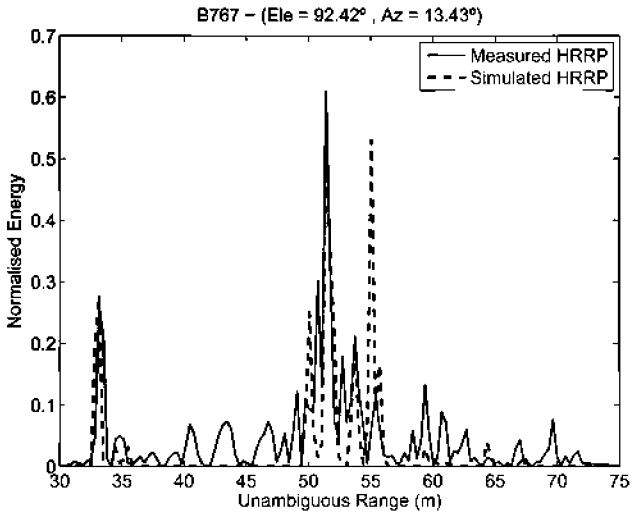

Fig. 4 *Difference between actual and synthetic range profiles*

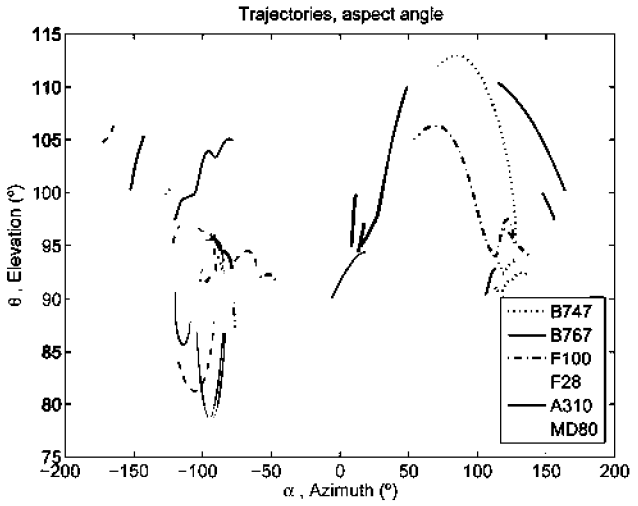

Fig. 5 *Described trajectories*

To validate the algorithm, HRRPs are grouped in frames. Each frame comprises sequences of profiles collected sequentially during the *ORFEO* measurement campaign, time-shift compensated [29] and with a variation in azimuth of 2.5°. A total number of 235 frames are extracted from the trajectories depicted in Fig. 5, where nose-on aspect angles correspond approximately to ($\theta = 90^\circ$, $\alpha = 0^\circ$). From these trajectories, 39 frames correspond to an A310, 42 to a B747, 43 to an F100, 34 to a B767, 38 to an F28, and 39 to an MD80. Even if the test set is not too large, the results will allow us to decide whether the algorithm is worthwhile to continue the research.

3 Experimental results

As stated, and in contrast to MSM, there is no need to set the subspace dimensionality in gMSM, however, it does exist the question about which value of m is best for the *softweighting*. Note that the higher the m is, the more eigenvectors are treated with a *softweight* of 1. This implies, on the one hand that the gMSM gets equivalent to MSM with large dimension of subspaces if m is very high; on the other hand, and highly related to the former statement, with a high value of m, eigenvectors representing the *noise subspace* will be probably considered as part of the *signal subspace*; this can cause the similarity between subspaces to be very close for all aircraft classes, thus, recognition performance can be negatively affected.

Accordingly, m is recommended to be set to low values. In order to clarify these assumptions, a study on the parameter m has been carried out. Firstly, m has been chosen dynamically for the test and training samples: if λ_i is the ith eigenvalue out of N, m is calculated (separately for test and training sets) according to a threshold η ($0 \leq \eta \leq 1$), such that

$$\arg\min_m \left(\left| \sum_{i=1}^{m} \lambda_i - \eta \cdot \sum_{i=1}^{N} \lambda_i \right| \right) \tag{8}$$

In Fig. 6*a*, the tendency of the recognition performance with the variation of m depending on η is presented. Different thresholds for test and training samples are set. Each curve in the figure depicts the evolution of the recognition rate according to a fixed threshold of the training set while varying the threshold of the test set. In Fig. 6*b* the mean value of m obtained for the test and training samples is depicted, that is, the equivalence between η and m. As seen in Fig. 6*b*, higher η means higher m and as the plot 6(a) shows, the recognition rates reach lower values with high η than those obtained with a lower one, that is with lower m. Consequently, and as already stated, m should be set to a low value.

As Fig. 6*a* depicts, with a value of $\eta = 0.6$ for the test samples and $\eta = 0.4$ for the training samples, the recognition rate reaches the highest value for this experiment (87.66%). On the other hand, Fig. 6*b* shows that with $\eta = 0.6$, the mean value of m for the test samples is close to 1 and with $\eta = 0.4$, is also practically 1 for the training samples. This means that some test samples will obtain better recognition results if $m > 1$ but normally with $m = 1$ the recognition is correctly accomplished.

Under the assumption of low m and after the analysis of Fig. 6, it seems fairly reasonable to set $m = 1$ in order to obtain good recognition results. Thus, applying gMSM to the frames that form the test set and setting $m = 1$ for the *softweighting*, the final identification rates obtained are shown in Table 2. The Table shows good recognition rates for all the aircraft in the test set, although the F28 is the one with the lowest rate because it is very similar to the F100 and it causes confusion when classifying some test samples. In any case, the error rates for all the aircraft are quite good (less than 20%) and globally, the average for all aircraft is less than 15% and the global recognition rate achieved is 87.2%. As Fig. 6*a* showed, the best recognition rate obtained with a dynamic value of m was higher than this one. Nevertheless, the tuning of parameter m needs a high computational cost, thus, in order to present a faster and more general algorithm with no need to be tuned every time a new test/training sample is introduced, m has eventually been set to a fixed value of unity.

In order to further assess the performance, the method is compared to three different algorithms: the first one is the MSM already described in Section 2.1; the second one is a subspace-based method presented in [30] where SVD is used to define the subspaces that will represent each target (with a threshold of 85%) and the algorithm used for identification is also based on angle between subspaces, although in this specific case, between a vector and a subspace with a weighting element; lastly, another subspace-based method presented in [4] is used for comparison, the PCA-based minimum reconstruction error approximation, where PCA is used to extract the feature subspace of a frame of HRRPs (with a threshold of 99%) and then, the algorithm decides the test sample class considering its minimum reconstruction error in the feature subspaces. The reader is referred to the cited papers for more information about the algorithms. Table 3 shows the comparative recognition results obtained for the aforementioned methods using the same test and training sets presented in this paper. The parameters selected for each algorithm are equal to the ones chosen in their respective references, that is for entry F2 in the Table, the threshold parameter for the subspace design is set to ($\eta = 0.85$)[30] and for entry F3 the threshold for the feature subspace formation is set to ($\eta = 0.99$) as [4] states. In the case of

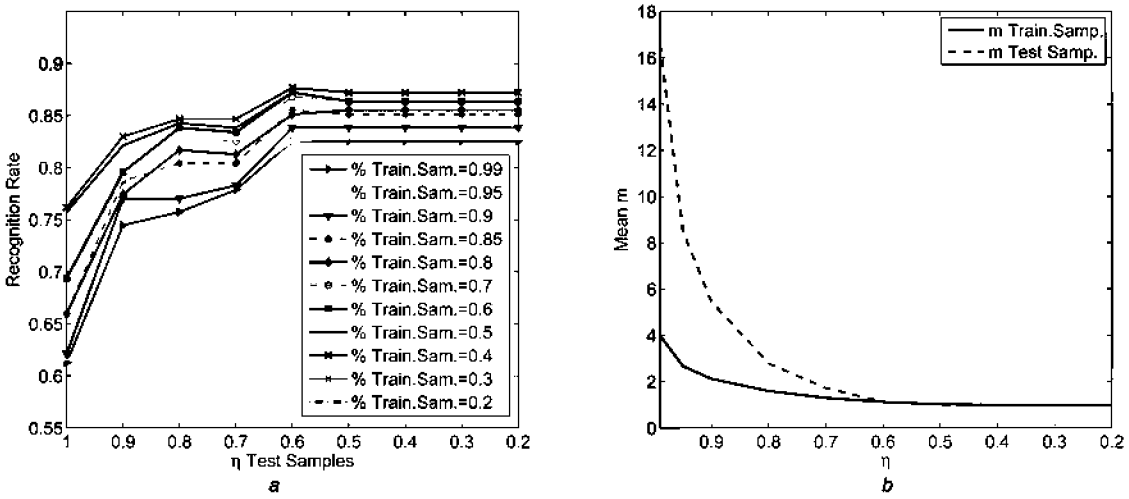

Fig. 6 *Parametric study of softweights*

a Recognition performance with dynamic softweights
b Mean m obtained according to η

Table 2 gMSM confusion matrix; $m = 1$

Class	A310	B747	F100	B767	F028	MD80	% Success	% Error
A310	36	0	0	2	1	0	92.3	7.7
B747	5	35	0	0	2	0	83.3	16.7
F100	0	0	37	0	5	1	86.0	14.0
B767	2	0	0	32	0	0	94.1	5.9
F028	0	0	6	0	31	1	81.6	18.4
MD80	2	0	1	2	0	34	87.2	12.8
avg. recog. rate							87.2	12.8

algorithm MSM the threshold is set to ($\eta = 0.85$) due to the similarity between this algorithm and F2.

An analysis of Table 3 shows that the gMSM with a value of $m = 1$ results in the highest average recognition rate (87.2%). The most basic method, since it does not add any weighting element and simply computes the angle between two subspaces, the MSM, returns the poorest results, an average recognition rate of 80%, as well as algorithm F2, related somehow to MSM but with additional weighting elements. The approach F3 outperforms F2 and MSM in approximately 6 percentage points, yet it does not reach the highest recognition rate, although it is only 1.1 percentage points lower.

Results have shown that gMSM method with a fixed value of parameter $m = 1$ achieves good recognition results compared to other algorithms, thus, it can be said that this method is appropriate for NCTI purposes. Remember the lack of resemblance between test and training sets: while synthetic profiles are 'clear' signatures of aircraft because they have been predicted with CAD models and under ideal conditions, actual profiles undergo the effects of noise and other unwanted information. Moreover, synthetic profiles are obtained under the assumption of trajectories being the ones followed by the measured aircraft, nevertheless, the aspect angles under which the actual targets are seen are just estimations; this fact adds more dissimilarities between actual and synthetic profiles, but on the other hand, it adds robustness to the algorithm since recognition rates are over 87%. Thus, considering the dissimilarities between profiles presented in this study and the high recognition rates obtained, the method can be considered as promising for NCTI purposes with HRRP.

Table 3 Average recognition rates for different algorithms

Class	gMSM ($m = 1$) %	MSM ($\eta = 0.85$) %	F2 [30] ($\eta = 0.85$) %	F3 [4] ($\eta = 0.99$) %
A310	92.3	89.7	92.3	94.1
B747	83.3	73.8	90.5	78.2
F100	86.0	72.1	72.1	79.8
B767	94.1	91.2	76.5	96.6
F028	81.6	81.6	78.9	68.8
MD80	87.2	74.4	69.2	94.4
avg. recog. rate	87.2	80.0	80.0	86.1

4 Conclusions

In this study a methodology for HRRP target recognition based on the MSM is shown. It has been proven that, in comparison to other methods, the introduction of weighting elements in the metrics returns higher recognition rates. Thus, by introducing *softweighting*, the gMSM assigns the importance of each basis in the subspace; target recognition is achieved according to the angle between these *softweighted*-subspaces with no need to previously set the subspace dimension unlike the original MSM. For the first time, gMSM has been proven to be a successful method to classify flying aircraft by means of a database of synthetic profiles. With the *softweighting*, an increase in the identification rates has been accomplished comparing with other methods. Moreover, the study of the evolution of the classification rates with the selection of parameter m to define the *softweights*, has shown that a fixed value of $m = 1$ is enough to obtain good results, nevertheless, should these results be further improved, a dynamic value for m must be set.

As noted, using a synthetic recognition database for the identification of actual measurements has been found to be problematic due to the dissimilarities between signatures. The input, which is measured under actual conditions, is affected by noise and other unwanted effects, while the synthetic profiles are the ideal signatures of aircraft replicas. These synthetic profiles

have been run considering their aspect angles as being the same as the actual measured profiles, nevertheless, these angles are mere predictions that may have an error up to 5°. This implies that the algorithm is valid even if the true aspect of the input differs in a few degrees from the aspect of the profiles stored in the database. Despite all these differences, the results obtained with the *softweighting* method are encouraging to further validate the algorithm accuracy and robustness with wider datasets.

5 Acknowledgment

The authors would like to thank the Spanish National Institute for Aerospace Technology (INTA) for the F.P.I. grant awarded to P.L.R. and also the members of NATO-RTO SET-112 Task Group on 'Advanced analysis and Recognition of Radar Signatures for Non-Cooperative Target Identification' for providing the actual data obtained in the measurement campaigns and used in this study as the test set. A special thanks is expressed to Juan Ángel Aguilar for his efforts in the CAD modelling.

6 References

1 Cohen, M.N.: 'An overview of radar-based, automatic, noncooperative target recognition techniques'. IEEE Int. Conf. on Systems Engineering, Dayton, OH, USA, August 1991, pp. 29–34
2 Wehner, D.R.: 'High-resolution radar' (Artech House, 1995, 2nd edn.)
3 Zwart, J.P., van der Heiden, R., Gelsema, S., *et al.*: 'Fast translation invariant classification of HRR range profiles in a zero phase representation', *IEE Proc. Radar Sonar Navig.*, 2003, **150**, (6), pp. 411–418
4 Du, L., Liu, H., Bao, Z., *et al.*: 'Radar automatic target recognition using complex high-resolution range profiles', *IET Radar Sonar Navig.*, 2007, **1**, (1), pp. 18–26
5 Li, H.-J., Yang, S.-H.: 'Using range profiles as feature vectors to identify aerospace objects', *IEEE Trans. Antennas Propag.*, 1993, **41**, (3), pp. 261–268
6 Bhatnagar, V., Shaw, A.K., Williams, R.W.: 'Improved automatic target recognition using singular value decomposition'. Proc. IEEE Int. Conf. on Acoustics, Speech and Signal Processing, Seattle, WA, May 1998, vol. 5, pp. 2717–2720
7 Kim, K.-T., Seo, D.-K., Kim, H.-T.: 'Radar target identification using one-dimensional scattering centres', *IEE Proc. Radar Sonar Navig.*, 2001, **148**, (5), pp. 285–296
8 Nan, C., Minghua, X.: 'Target recognition based on the self-correlation function of HRRP'. Int. Conf. on Electrical and Control Engineering (ICECE), Wuhan, China, June 2010, pp. 4787–4789
9 Zhou, D., Shen, X., Yang, W.: 'Radar target recognition based on fuzzy optimal transformation using high-resolution range profile', *Pattern Recognit. Lett.*, 2013, **34**, (3), pp. 256–264
10 Du, L., Liu, H., Bao, Z.: 'Radar HRRP statistical recognition: parametric model and model selection', *IEEE Trans. Signal Process.*, 2008, **56**, (5), pp. 1931–1944
11 Du, L., Liu, H., Wang, P., *et al.*: 'Multitask factor analysis with application to noise robust radar HRRP target recognition'. IEEE Radar Conf. (RADAR), Atlanta, GA, May 2012, pp. 202–207
12 Zhu, F., Zhang, X.-D., Hu, Y.-F., *et al.*: 'Nonstationary hidden Markov models for multiaspect discriminative feature extraction from radar targets', *IEEE Trans. Signal Process.*, 2007, **55**, (5), pp. 2203–2214
13 Liao, X., Runkle, P., Carin, L.: 'Identification of ground targets from sequential high-range-resolution radar signatures', *IEEE Trans. Aerosp. Electron. Syst.*, 2002, **38**, (4), pp. 1230–1242
14 Nelson, D.E., Starzyk, J.A., Ensley, D.D.: 'Iterated wavelet transformation and signal discrimination for HRR radar target recognition', *IEEE Trans. Syst. Man Cybern. A*, 2003, **33**, (1), pp. 52–57
15 Guo, Z., Li, S.: 'One-dimensional frequency-domain features for aircraft recognition from radar range profiles', *IEEE Trans. Aerosp. Electron. Syst.*, 2010, **46**, (4), pp. 1880–1892
16 Zyweck, A., Bogner, R.E.: 'Radar target classification of commercial aircraft', *IEEE Trans. Aerosp. Electron. Syst.*, 1996, **32**, (2), pp. 598–606
17 Shaw, A.K., Paul, A.S., Williams, R.: 'Eigen-template-based HRR-ATR with multi-look and time-recursion', *IEEE Trans. Aerosp. Electron. Syst.*, 2013, **49**, (4), pp. 2369–2385
18 Hotelling, H.: 'Relations between two sets of variates', *Biometrika*, 1936, **28**, pp. 321–377
19 Li, F., Dai, Q., Xu, W., *et al.*: 'Weighted subspace distance and its applications to object recognition and retrieval with image sets', *IEEE Signal Process. Lett.*, 2009, **16**, (3), pp. 227–230
20 Fukui, K., Yamaguchi, O.: 'Face recognition using multi-viewpoint patterns for robot vision'. The Eleventh Int. Symp. Robotics Research (ISRR), Siena, Italy, October 2003, pp. 192–201
21 Oja, E.: 'Subspace methods of pattern recognition', (*Electronic & Electrical Engineering Research Studies: Pattern Recognition and Image Processing Series*, **6**) (Research Studies Press, 1983)
22 Yamaguchi, O., Fukui, K., Maeda, K.: 'Face recognition using temporal image sequence'. Third IEEE Int. Conf. on Automatic Face and Gesture Recognition, Nara, Japan, April 1998, pp. 318–323
23 Bjoerck, A., Golub, G.H.: 'Numerical methods for computing angles between linear subspaces', *Math. Comput.*, 1973, **27**, pp. 579–594
24 Golub, G.H., Van Loan, C.F.: 'Matrix computations' (Johns Hopkins University Press, 1996, 3rd edn.)
25 Pasala, K.M., Malas, J.A.: 'HRR radar signature database validation for ATR: an information theoretic approach', *IEEE Trans. Aerosp. Electron. Syst.*, 2011, **47**, (2), pp. 1045–1059
26 Kobayashi, T.: 'Generalized mutual subspace based methods for image set classification'. Computer Vision ACCV 2012, 2013 (*LNCS*), **7724**, pp. 578–592
27 van der Heiden, R., de Vries, J.: 'The ORFEO measurement campaign. TNO Report'. TNO Defence, Security and Safety Report, FEL-96-A073, The Hague, The Netherlands, 1996
28 Perez, J., Catedra, M.F.: 'Application of physical optics to the RCS computation of bodies modeled with NURBS surfaces', *IEEE Trans. Antennas Propag.*, 1994, **42**, (10), pp. 1404–1411
29 Jeong, H.-R., Kim, H.-T., Kim, D.-H.: 'Application of subarray averaging and entropy minimization algorithm to stepped-frequency ISAR autofocus', *IEEE Trans. Antennas Propag.*, 2008, **56**, (4), pp. 1144–1154
30 López-Rodríguez, P., Escot-Bocanegra, D., Fernández-Recio, R., *et al.*: 'Non-cooperative target recognition by means of singular value decomposition applied to radar high resolution range profiles', *Sensors*, 2015, **15**, pp. 422–439